Photoelectron Spectroscopy of Singly and Doubly Charged Higher Fullerenes at Low Temperatures: C_{76}^-, C_{78}^-, C_{84}^- and C_{76}^{2-}, C_{78}^{2-}, C_{84}^{2-}†

Xue-Bin Wang,‡ Hin-Koon Woo,‡ Jie Yang,‡ Manfred M. Kappes,*,§ and Lai-Sheng Wang*,‡

Department of Physics, Washington State University, 2710 University Drive, Richland, Washington 99354, Chemical & Materials Sciences Division, Pacific Northwest National Laboratory, MS K8-88, P.O. Box 999, Richland, Washington 99352, and Institut für Physikalische Chemie, Universität Karlsruhe, Kaiserstrasse 12, D-76128 Karlsruhe, Germany

Received: January 16, 2007; In Final Form: March 29, 2007

Photoelectron spectroscopy of vibrationally cold singly and doubly charged higher fullerenes, C_n^- and C_n^{2-} (n = 76, 78, and 84), has been investigated at several photon energies. Vibrationally resolved spectra are obtained for both the singly and doubly charged species, and for n = 78 and 84, transitions from different isomers are also observed. The electron affinities (EAs) of C_{76}, C_{78}, and C_{84} are accurately determined to be 2.975 ± 0.010 eV for C_{76}, 3.20 ± 0.01 eV for $C_{78}(C_{2v})$, 3.165 ± 0.010 eV for $C_{78}(D_3)$, 3.23 ± 0.02 for $C_{78}(C_{2v}')$, 3.185 ± 0.010 eV for $C_{84}(D_2)$, and 3.26 ± 0.02 eV for $C_{84}(D_{2d})$. The second EA of the higher fullerenes, which represent the electronic stability of the doubly charged anions, are measured to be 0.325 ± 0.010 eV for C_{76}, 0.44 ± 0.02 eV for $C_{78}(C_{2v})$, 0.53 ± 0.02 eV for $C_{78}(D_3)$, 0.60 ± 0.04 eV for $C_{78}(C_{2v}')$, 0.615 ± 0.010 eV for $C_{84}(D_{2d})$, and 0.82 ± 0.01 eV for $C_{84}(D_2)$. The spectra of the dianions are observed to be similar to those of the singly charged anions, suggesting that the charging induces relatively small structural changes to the fullerene cages. The onsite Coulomb repulsions in the doubly charged fullerenes are directly measured from the differences of the first and second EAs and reveal strong correlation effects between the two extra electrons. The repulsive Coulomb barriers in the doubly charged fullerenes are estimated from the cutoff in the photoelectron spectra and are found to be consistent with estimates from an electrostatic model.

1. Introduction

The intrinsic properties of isolated multiply charged anions (MCAs) have attracted much attention during the past decade.[1−5] The electronic stability of an MCA is dictated by the electron binding ability of the corresponding neutral molecule and the Coulomb repulsion between the excess charges. Fullerenes possess high electron affinities (EAs) and are capable of accepting multiple electrons in the condensed phases. The electronic structures, electron−electron, and electron−phonon interactions of multiply charged fullerene anions are important for the superconductivity in doped fullerides.[6,7] Small fullerene dianions (C_{60}^{2-} and C_{70}^{2-}) are among the first dianions observed in the gas phase by mass spectrometry.[8,9] They have subsequently been produced by electron attachment to C_{70}^- in a Penning trap,[10] as well as by charge transfer from Na to C_{60}^- and C_{70}^- very recently.[11,12] Theoretical calculations and lifetime measurement indicate that C_{60}^{2-} is unstable and short-lived with the second electron affinity (EA2) of C_{60} being negative (−0.3 eV).[6,8,12] Very recently, C_{70}^{2-} has been confirmed to be the smallest stable fullerene dianion in the gas phase with an adiabatic detachment energy (ADE) of +0.02 eV by photoelectron spectroscopy (PES) of vibrationally cold C_{70}^{2-} dianions.[13]

The stabilities of the fullerene dianions are expected to increase with the fullerene cage size, and indeed higher fullerene dianions, C_n^{2-} (n = 76, 78, 84), were readily generated by electrospray ionization (ESI).[14,15] Their PES spectra have been reported recently.[16,17] The ADEs of the dianions were observed to be positive and increase with the fullerene size as expected. However, the previous PES spectra were taken at relatively low resolution under room temperature. The high internal energy distributions inherent in these relatively large molecular dianions resulted in long tails in the PES spectra, which complicated the determination of the ADEs and generally led to lower ADE values. For example, the extrapolated ADE of C_{70}^{2-} based on the reported ADEs of C_{76}^{2-}, C_{78}^{2-}, and C_{84}^{2-} was −0.28 eV,[17] which was lower than the real ADE of C_{70}^{2-} by ∼0.3 eV.[13]

Using a recently developed low-temperature ESI-PES apparatus, the photoelectron spectroscopy of vibrationally cold C_{60}^- has been obtained,[18] which led to the accurate measurement of the first EA of C_{60} (2.683 eV). Using this apparatus, we have also obtained the PES spectra of vibrationally cold C_{70}^- and C_{70}^{2-}, allowing the first and second EA of C_{70} to be accurately determined, as 2.765 and 0.02 eV, respectively.[13] Here we report a PES study of vibrationally cold singly and doubly charged higher fullerene anions C_n^{2-} and C_n^- (n = 76, 78, 84) using the low-temperature ESI-PES apparatus. PES spectra have been obtained at several photon energies, ranging from 6.424 eV (193 nm) to 532 nm (2.331 eV), allowing more accurate measurements of the first and second EAs of the higher fullerenes, as well as the repulsive Coulomb barriers (RCBs) in the dianions. The patterns of the PES spectra of the doubly charged fullerene anions C_n^{2-} are observed to be similar to those of the corresponding singly charged species C_n^- except for a red shift of ∼2.6 eV due to the intramolecular Coulomb repulsion in the dianions. For C_{78} and C_{84}, the higher resolution PES spectra

† Part of the special issue "Richard E. Smalley Memorial Issue".

* Corresponding authors. E-mail: Manfred.Kappes@chemie.uni-karlsruhe.de and ls.wang@pnl.gov.

‡ Washington State University and Pacific Northwest National Laboratory.

§ Universität Karlsruhe.

10.1021/jp0703861 CCC: $37.00
Published on Web 05/17/2007

also allowed information for different isomers to be obtained for both the singly and doubly charged anions.

2. Experimental Details

The experiments were carried out with a newly built low-temperature instrument that couples an ESI source to a magnetic-bottle PES analyzer.[18,19] The ESI source and the PES analyzer are similar to those described previously.[20] A key feature of the new instrument is its cooling capability, accomplished by attaching the cold head of a close cycle helium refrigerator to an ion trap where ions are accumulated and cooled via collisions with a cold background gas. The C_{78}^{m-} and C_{84}^{m-} ($m = 1, 2$) anions were formed in solution via bulk chemical reduction of neutral C_{78} and C_{84} by a reducing agent (propanethiol).[21] The same procedure was not able to generate enough anions of C_{76}^{m-}, which were successfully produced using tetrakis(dimethylamino)ethylene (TDAE) as the reducing agent in *o*-dichlorobenzene solvent, as described before.[14] The solutions containing the fullerene anions and the reducing agents were used directly in the electrospray. The anions produced from the ESI source were guided by a rf-only octopole into a quadrupole mass filter operated in the rf-only mode. Following the mass filter, ions were directed by a 90° ion bender to a temperature-controlled ion trap, where they were accumulated and cooled for 0.1 s before being pulsed out into the extraction zone of a time-of-flight mass spectrometer. For the current experiment, the ion trap was operated at 70 K and approximately 0.1 mTorr N_2 was used as the background gas. Previous experiments suggested that a 70 K nominal trap temperature corresponded to an effective ion temperature of about 70−100 K,[18,19] which was sufficient to remove hot band transitions in the PES spectra of C_{60}^- and C_{70}^- and allowed vibrationally resolved spectra to be obtained.[13,18]

During the PES experiment, anions of interest were mass selected and decelerated before being intercepted by a detachment laser beam in the interaction zone of a magnetic-bottle photoelectron analyzer. Four photon energies were used in the current study: 193 nm (6.424 eV) from an ArF excimer laser and 266 nm (4.661 eV), 355 nm (3.496 eV), and 532 nm (2.331 eV) from a Nd:YAG laser. The lasers were operated at a 20 Hz repetition rate with the ion beam off at alternate shots for background subtraction. Photoelectrons were collected with high efficiency by the magnetic bottle and analyzed in a 5.2 m long electron flight tube. Photoelectron time-of-flight spectra were collected and then converted into kinetic energy spectra, calibrated by the known spectra of I^- and ClO_2^-. Electron binding energy spectra were obtained by subtracting the kinetic energy spectra from the detachment photon energies, followed by a constant energy smoothing procedure (5 meV for 266 nm, 10 meV for 193 nm). The energy resolution ($\Delta E/E$) was estimated to be approximately 2%, i.e., approximately 20 meV for 1 eV electrons.

3. Results

Both the doubly and singly charged higher fullerene anions C_n^{2-} and C_n^- ($n = 76,78,$ 84) are readily produced in our ESI source. Two C_{78} samples were sprayed: one sample, designated as C_{78}(all), was a non-isomer-separated sample containing three isomers, C_{2v}, C_{2v}', and D_3, and a second sample was D_3-enriched and was designated as $C_{78}(D_3)$.[17,22,23] The spectra of all the singly charged anions were taken at three photon energies, 355, 266, and 193 nm, and those of the dianions were all measured at four different photon energies, 532, 355, 266, and 193 nm. Figures 1−4 show the PES spectra of C_n^- (left column) and C_n^{2-} (right column) for $n = 76$, 78(all), 78(D_3), and 84, respectively. The ADEs of C_n^- and C_n^{2-}, or the EA1 and EA2 of the neutral fullerenes, as well as other spectroscopic constants obtained, are summarized in Tables 1 and 2, respectively.

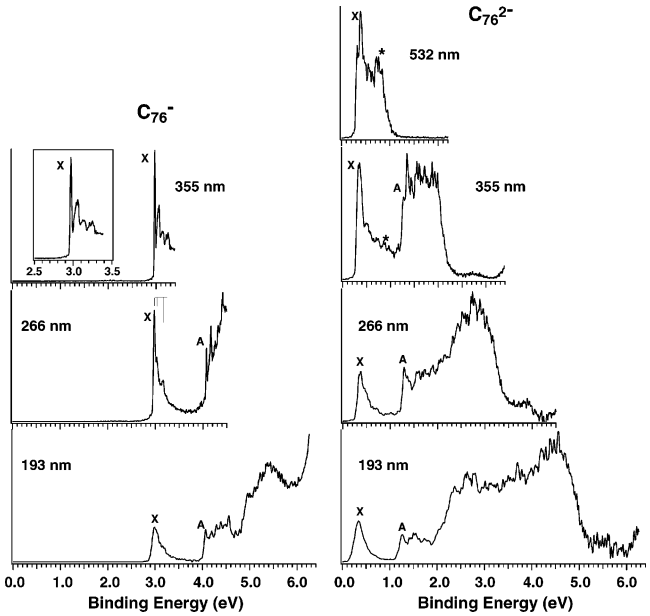

Figure 1. Photoelectron spectra of vibrationally cold C_{76}^- (left) and C_{76}^{2-} (right). The insert is an expanded view of the 355 nm spectrum of C_{76}^-. The resolved vibrational progressions are indicated in the 266 nm spectrum of C_{76}^-. Asterisk indicates features due to shakeup.

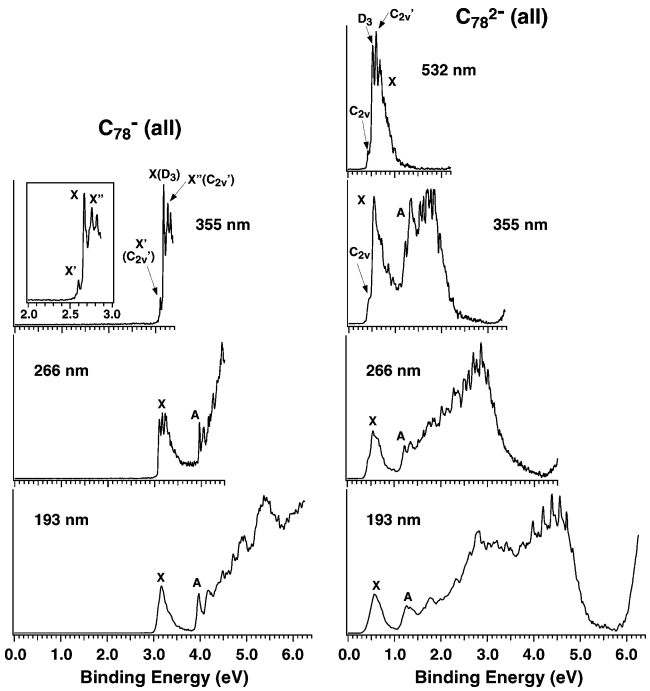

Figure 2. Photoelectron spectra of vibrationally cold C_{78}^- (left) and C_{78}^{2-} (right) from an as-extracted C_{78} sample. The insert is an expanded view of the 355 nm spectrum of C_{78}^-.

3.1. C_{76}^- and C_{76}^{2-}. 3.1.1. C_{76}^-. Figure 1 shows the PES spectra of C_{76}^- (left) recorded at the three photon energies. C_{76} is known to exist in only one isomer with D_2 symmetry, as extracted from the fullerene soot.[23] The 193 nm spectrum of C_{76}^- reveals a low binding energy feature (X), followed by a band gap and a series of congested high binding energy features. At 355 nm, only the ground state (X) is accessible, whereas at 266 nm, both the ground (X) and the first excited state (A) are

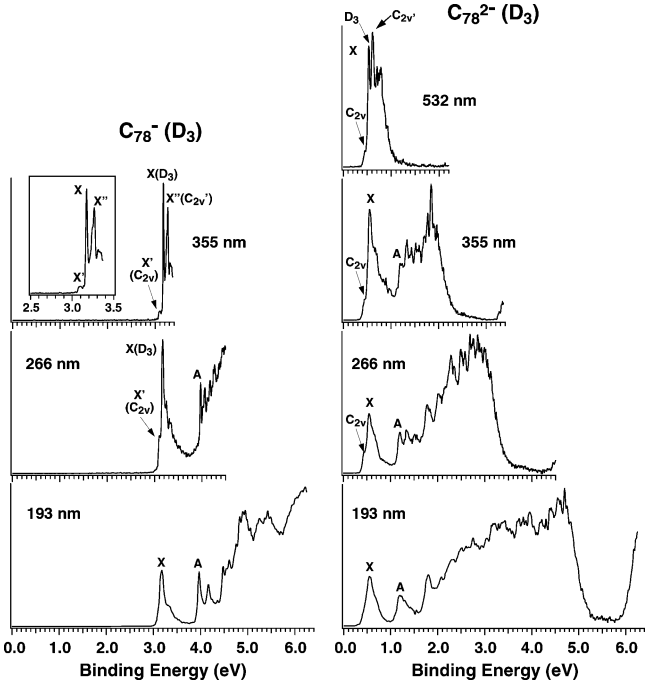

Figure 3. Photoelectron spectra of vibrationally cold C_{78}^- (left) and C_{78}^{2-} (right) from a D_3-isomer-enriched C_{78} sample. The insert is an expanded view of the 355 nm spectrum of C_{78}^-.

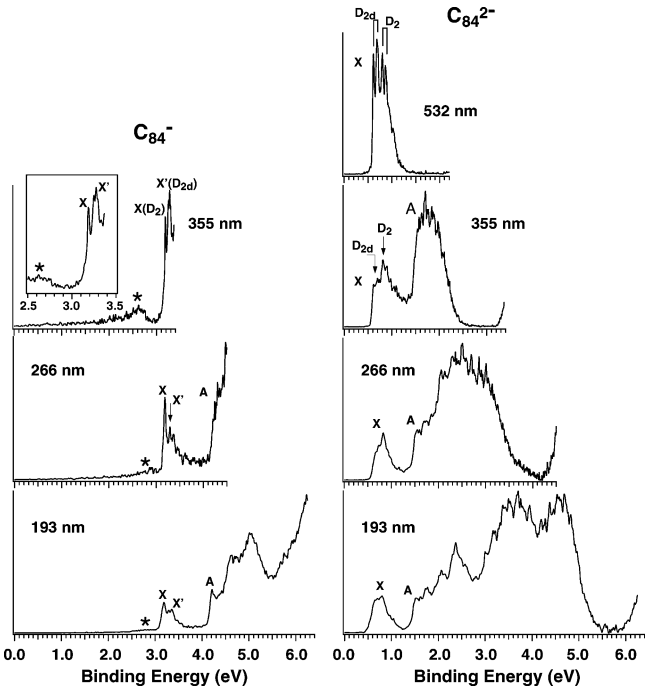

Figure 4. Photoelectron spectra of vibrationally cold C_{84}^- (left) and C_{84}^{2-} (right). The insert is an expanded view of the 355 nm spectrum of C_{84}^-. The weak signals (*) on the low binding side of the C_{84}^- spectra are due to an unidentified impurity from the C_{84}^- beam.

observed. Vibrational structures are resolved for the ground state (X) of C_{76} at 355 and 266 nm. It appears that sharp vibrational features are also resolved for the first excited state (A) of C_{76} in the 266 nm spectrum. The vibrationally resolved features allow accurate measurements of the EA and the excitation energy for the first excited-state of C_{76} as 2.975 ± 0.010 and 1.10 ± 0.01 eV, respectively. The excitation energy is also an approximate measure of the energy gap between the highest occupied molecular orbital (HOMO) and the lowest unoccupied molecular orbital (LUMO) of C_{76}. Two vibrational progressions

TABLE 1: The Measured First Electron Affinities (EAs) and HOMO−LUMO Gaps of the Higher Fullerene C_n (n = 76, 78, 84) Compared to Those of C_{60} and C_{70}[a]

	EA (eV)		
	this work	refs	HOMO−LUMO (eV)
C_{60}		2.683(0.008)[b]	1.62[b]
C_{70}		2.765(0.010)[c]	1.55[d]
C_{76}	2.975(10)	2.89(5)[d]	1.10(1)
C_{78} (C_{2v})	3.10(1)	3.10(6)[d]	
C_{78} (D_3)	3.165(10)		0.80(1)
C_{78} (C_{2v}')	3.23(2)		
C_{84} (D_2)	3.185(10)	3.14(6)[d]	~1.02
C_{84} (D_{2d})	3.26(2)		

[a] Numbers in parentheses represent the experimental uncertainties in the last digit. [b] Reference (18). [c] Reference (13). [d] Reference (30), not isomer-specific for C_{78} and C_{84}.

TABLE 2: Experimental Adiabatic Detachment Energies (ADEs), Onsite Electron−Electron Interactions (Onsite (e−e)), and Repulsive Coulomb Barrier (RCB) for the Fullerene Dianions C_n^{2-} (n = 70, 76, 78, 84)[a]

	ADE[b]			
	this work	refs	onsite (e−e)[d]	RCB (exp)
C_{70}^{2-}		0.02[c]	2.745[c]	1.6[c]
C_{76}^{2-}	0.325(10)	0.08(10)[e]	2.65	1.5
C_{78}^{2-} (C_{2v})	0.44(2)	0.15(15)[e]	2.66	
C_{78}^{2-} (D_3)	0.53(2)		2.64	1.5
C_{78}^{2-} (C_{2v}')	0.60(3)		~2.62	
C_{84}^{2-} (D_{2d})	0.615(10)	0.41(7)[e]	2.65	1.4
C_{84}^{2-} (D_2)	0.82(1)		2.37	

[a] All energies are in eV. Numbers in parentheses represent the experimental uncertainties in the last digit. [b] Also represent the experimental second electron affinity (EA2) of the corresponding neutral fullerenes. [c] Reference 13. [d] Calculated from the differences of the first and second electron affinity (EA1 − EA2) of the corresponding fullerene neutral molecules. [e] Ref 17.

are resolved for the ground state transition (X) with frequencies of 440 and 1490 cm^{-1}. Similar vibrational frequencies (436 and 1451 cm^{-1}) have been estimated from Raman spectroscopy for the ground electronic state of C_{76}.[24] The vibrational structures in the 355 nm spectrum reveal that the three peaks at the high binding energy side are significantly broader than the 0−0 transition, possibly due to overlap of many vibrational modes, as is the case in the PES spectrum of C_{60}^-.[18]

3.1.2. C_{76}^{2-}. The PES pattern of C_{76}^{2-} is generally similar to that of C_{76}^-, except that C_{76}^{2-} exhibits much lower electron binding energies due to the strong intramolecular Coulomb repulsion between the two excess electrons. The X−A (HOMO−LUMO) gap is measured to be 0.93 eV, slightly smaller than that of C_{76}^-, suggesting that the filling of the two electrons in the LUMO of C_{76} does not induce significant structural changes to the fullerene cage or cause significant electron relaxation. The X−A band gap region is relatively clean in the 193 and 266 nm spectra but is filled with some continuous signals in the 355 nm spectrum. These signals in the band gap region seem to increase with decreasing photon energies, forming a peak (*) at 0.7 eV in the 532 nm spectrum. These signals are likely due to multielectron transitions (shape up), as will be discussed in section 4.3 below. At 532 nm, a sharp peak at the rising edge of band X is resolved, which should represent the 0−0 transition and yield an accurate ADE for C_{76}^{2-} (or EA2 of C_{76}) as 0.325 ± 0.010 eV.

In each spectrum of C_{76}^{2-} (Figure 1, right column), there is a cutoff at the high binding energy side due to the RCB, which universally exists for removing an electron from an MCA and prohibits slow photoelectrons with kinetic energies less than

the RCB from being emitted.[4,5] The RCB can be approximately estimated from this cutoff.[25,26] The cutoffs occur at ~0.8, ~2.0, ~3.1, and ~4.9 eV electron binding energies in the 532, 355, 266, and 193 nm spectra, respectively, yielding a RCB height of ~1.5 eV consistently at all four photon energies.

3.2. C_{84}^- and C_{84}^{2-}. 3.2.1. C_{84}^-. Two isomers (D_2 and D_{2d}) are known to exist with a ratio of 2:1 in the as-extracted C_{84} sample,[17] which is expected to lead to some complications in the PES spectra of C_{84}^- and C_{84}^{2-}. The spectra of C_{84}^- at 266 and 193 nm (Figure 4, left column) show several low binding energy features between 3.1 and 3.5 eV, followed by an energy gap and more congested features beyond the A band at 4.2 eV. The low binding energy features consist of multiple peaks with their relative intensities dependent on the photon energies, consistent with the presence of multiple isomers. The threshold peak (X) is the main peak in the 266 and 193 nm spectra in the low binding energy range, but its relative intensity is reduced in the 355 nm spectrum. The peak labeled with X′ becomes the dominant peak in the 355 nm and it is relatively broad with fine features (see the insert in Figure 4). Therefore, the X and X′ peaks should represent transitions from two different isomers. The width of the X′ peak suggests that it may contain overlapping vibrational transitions from the X band. We assign the lower binding energy peak (X) to the D_2 isomer and the X′ peak to the D_{2d} isomer according to their relative intensities in the 266 and 193 nm spectra. The resolved fine features in the low binding energy range beyond the X′ peak in the 266 nm should be due to vibrational transitions from both isomers. Thus, the X peak defines the EA for the D_2 isomer of C_{84} as 3.185 ± 0.010 eV, whereas the X′ peak defines the EA for the D_{2d} isomer of C_{84} as 3.26 ± 0.02 eV. If we assign the A band to be mainly from the D_2 isomer, we obtain a HOMO−LUMO gap for the D_2−C_{84} as 1.02 eV. The HOMO−LUMO gap for the D_{2d} isomer should be similar or slightly smaller. Very weak signals below 3.0 eV (labeled "*") are observed in the spectra of C_{84}^-. Similar signals are not detected in the spectra of C_{84}^{2-}, and they are likely due to an unidentified impurity in the C_{84}^- beam.

3.2.2. C_{84}^{2-}. While the spectra of C_{84}^{2-} (Figure 4, right column) exhibit similar spectral patterns to that of C_{84}^-, the low binding energy range between 0.5 and 1.1 eV becomes more congested due to the presence of the D_2 and D_{2d} isomers. The presence of the two isomers is quite apparent in the 355 and 266 nm spectra, where two sets of peaks with different intensities are partially resolved. We attribute the more intense part with slightly higher binding energies to the D_2 isomer, and the slightly weak and lower binding energy part to the D_{2d} isomer. These two spectral parts are resolved into four relatively sharp vibronic peaks in the 532 nm spectrum, allowing the EA2 of C_{84} or the ADE of C_{84}^{2-} to be fairly accurately determined: 0.615 ± 0.010 eV for the D_{2d} isomer and 0.815 ± 0.010 eV for the D_2 isomer. The band gap in C_{84}^{2-}, which seems to be slightly reduced compared to that in C_{84}^-, cannot be estimated because we cannot unambiguously correlate the higher binding energy transitions to a given isomer. The high binding energy spectral cutoffs occur at ~0.9, 2.1, 3.0, and 5.0 eV in the 532, 355, 266, and 193 nm spectra, respectively, yielding a RCB height for C_{84}^{2-} to be ~1.4 eV.

3.3. C_{78}^- and C_{78}^{2-}. The as-extracted C_{78} sample from the fullerene soot is known to contain three isomers: D_3, C_{2v}, and C_{2v}' isomers,[17,22,23] which are expected to yield very complicated PES spectra with overlapping transitions from all three isomers. Thus, to help spectral identification, we carried out PES experiments on an as-extracted sample [C_{78}(all)] (Figure 2) and a D_3-enriched sample [$C_{78}(D_3)$] (Figure 3).

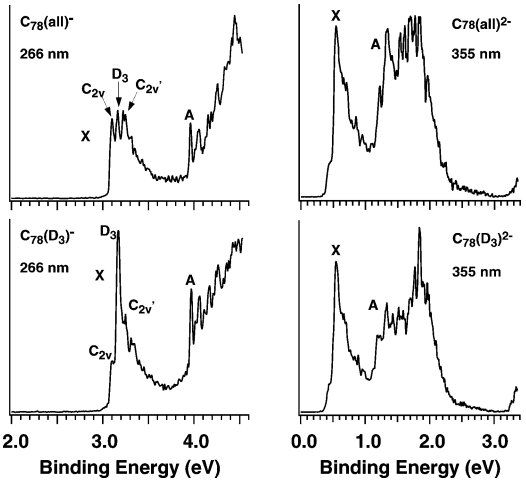

Figure 5. Comparison of 355 nm spectra of C_{78}^{2-}(all) vs $C_{78}^{2-}(D_3)$, and the 266 nm spectra of C_{78}^-(all) vs $C_{78}^-(D_3)$.

3.3.1. C_{78}^-. The cold anions and the improved PES resolution allow transitions from different isomers to be clearly resolved in the ground state region in the spectra of C_{78}^-, particularly in the 355 and 266 nm spectra (Figures 2 and 3). The D_3-enriched sample provides key information for the isomer assignments. Major differences are observed for the two C_{78}^- samples in the 266 nm spectra, as compared in Figure 5 (left column). Three peaks with about equal intensities are observed in the low binding energy region in the C_{78}(all) sample, but the $C_{78}(D_3)$ sample shows a dominating peak, which should be due to the D_3 isomer of C_{78}^-. The threshold peak is significantly weakened in the $C_{78}(D_3)$ sample; its intensity is also reduced in the 355 nm spectra. This feature is assigned to the C_{2v} isomer because previous UV−vis absorption studies suggest that among the three isomers the C_{2v} isomer possesses the largest HOMO−LUMO gap,[22] which usually means a lower EA for the neutral species. Therefore, the peak on the higher binding energy side in the low binding energy region in the 266 nm spectrum of C_{78}(all)$^-$ should be due to the C_{2v}' isomer of C_{78}^-. Thus, the EAs of C_{78} are determined to be 3.10, 3.165, and 3.23 eV for the C_{2v}, D_3, and C_{2v}' isomers, respectively, from the well-resolved ground-state transitions.

Sharp peaks are also resolved in the excited-state region (A) beyond the band gap. The peak at 3.98 eV should come from the D_3 isomer, yielding a HOMO−LUMO gap for the D_3 C_{78} as 0.80 eV. The excited-state features for the C_{2v} and C_{2v}' isomers are difficult to assign unambiguously.

3.3.2. C_{78}^{2-}. For C_{78}^{2-}, it is surprising that there are no significant changes in the low binding energy region in the PES spectra at all four photon energies between the two samples (Figures 2 and 3, right columns). The higher binding energy region beyond the band gap does show some difference between the two samples, as compared for the 355 nm spectra in Figure 5 (right column). Our observations seem to be consistent with the previous ESI and PES study,[17] which suggests that among the three isomers of C_{78} only the C_{2v} isomer forms dianions efficiently, the C_{2v}' isomer does not form dianions, and the D_3 isomer forms dianion less efficiently than the C_{2v} isomer. However, the current improved PES data for C_{78}^{2-} indicate that all three isomers are present, except that one of them is dominating and the dominating isomer is the same in both samples. Furthermore, we observe that the spectral pattern in the ground state region of the C_{78}^{2-} spectra is very similar to that in the spectra of the $C_{78}(D_3)^-$ singly charged anion. Thus, it seems reasonable to assign the dominating isomer in the

current experiment to be the D_3 isomer, which disagrees with the previous assignment of the C_{2v} isomer as the dominating dianion species.[17] One of the reasons for the previous assignment is that the PES spectrum from a D_3-enriched sample could not be distinguished from that from a C_{2v}-enriched sample. Thus the dianions from the D_3-enriched sample were assumed to come from the C_{2v} impurity in the D_3-enriched sample. Since the PES spectra of the three isomers are fairly similar, the previous lower resolution spectra would not have been able to distinguish between the two isomers. According to our current assignments, the second EAs of the three C_{78} isomers are in the same order as the first EAs. And the EA2s of C_{78} or the ADEs of C_{78}^{2-} are measured to be 0.44, 0.53, and 0.60 eV for the C_{2v}, D_3, and C_{2v}' isomers, respectively, from the well-resolved low photon energy spectra shown in Figures 2 and 3.

It is more difficult to make any definitive assignments for the different isomers in the higher binding energy region. In general, the band gaps seem to be slightly reduced in the dianions relative to that in the singly charged anions. Spectral cutoffs are observed in all the C_{78}^{2-} spectra in the high binding energy side due to the RCB, which is estimated to be about 1.5 eV.

4. Discussion

4.1. The Electronic Structure of the Higher Fullerenes. Like C_{60} and C_{70}, the higher fullerenes C_n (n = 76, 78, 84) are highly stable, closed-shell, caged allotropes of carbon. The extra electrons in the anions are expected to reside in the LUMO of the neutral species without inducing significant structural changes, which is reflected by the similar spectral patterns between the dianions and the singly charged anions. The PES spectra directly reveal the HOMO−LUMO gaps. In general, we observe that the band gaps in the dianions are slightly smaller than those in the singly charged anions due to the electronic relaxation effects. The HOMO−LUMO gaps in the higher fullerenes (Table 1) are all significantly smaller than that in C_{60} (1.62 eV) or C_{70} (1.55 eV), in accord with the observed fullerene abundance and their expected electronic stability.

In the previous PES study on the higher fullerene doubly charged anions,[17] time-dependent density-functional calculations were performed to simulate the PES spectra and compare with the experimental data. The LUMOs of all the isomers of C_{76}, C_{78}, and C_{84} were found to be nondegenerate, except the D_{2d} isomer of C_{84} that possesses a doublet degenerate LUMO. Thus, the doubly charged anions of the three higher fullerenes should be singlet state and the D_{2d} C_{84}^{2-} should be a triplet. The simulated PES spectra are in general in good agreement with the current higher resolution spectra. Specifically, spectra for all three isomers of C_{78}^{2-} were simulated. The first excited state of the singly charged anions was found to be at 0.755 eV for the D_3 isomer and 1.064 eV for the C_{2v} isomer. The previous work concluded that the simulated spectrum of the C_{2v} isomer agreed best with the then low-resolution data. However, we find that both the first excited-state energy and the simulated spectrum for the D_3 isomer in fact agree better with the current higher resolution spectra of C_{78}^{2-}, providing considerable credence for the current isomer assignments.

4.2. The First and Second Electron Affinities of Higher Fullerenes and the Stability of Their Doubly Charged Anions. Fullerenes are known to be remarkable electron acceptors due to their spherical delocalized π LUMOs and all exhibit very high EAs.[27,28] For example, C_{60} can be doped with up to six alkali metals to form C_{60}^{6-} fullerides in the condensed phase to fill up the triplet degenerate LUMO[6] and has been demonstrated in multiple distinct redox steps in electrochemical processes.[29] As compared in Table 1, the EA of the fullerenes increases with the cage size. We have measured the EAs of C_{60} (2.683 eV)[18] and C_{70} (2.765 eV)[13] fairly accurately before. The EAs of the higher fullerenes are all higher, even though there is a slight variation among the different isomers for C_{78} and C_{84} (Table 1). A previous study using charge exchange reactions determined the EAs for C_{76}, C_{78}, and C_{84},[30] which are compared with the current values in Table 1. In addition to giving more accurate EAs, the current PES study also yields isomer-specific information.

The second EA (EA2) or the stability of the doubly charged fullerenes also increases with the cage size. While we showed previously that C_{70}^{2-} is barely stable with an ADE of 0.02 eV,[13] the larger fullerenes all possess significant EA2 (Table 2) and are highly stable species in the gas phase. As compared in Table 2, the current study yields more accurate and higher EA2s than the previous study at room temperature,[17] due to the elimination of vibrational hot bands and higher spectral resolution.

4.3. The Onsite Coulomb Repulsion in Doubly Charged Fullerenes. Electron−electron repulsion and exchange interactions, which are essential many-body effects in molecular and solid-state physics, are particularly important for multiply charged anions. As shown in our previous PES study of C_{70}^{2-},[13] fullerene dianions are ideal systems to study electron−electron (e−e) interactions because the two extra electrons are delocalized over the molecular cages and well separated in energy from that of the "neutral core". The difference between EA1 and EA2 represents the e−e interaction energy on the fullerene cage and is a direct measure of the onsite Coulomb repulsion. As given in Table 2, the onsite Coulomb repulsions for the higher fullerene dianions are 2.65 (C_{76}), 2.66 (C_{78}, C_{2v}), 2.64 (C_{78}, D_3), 2.62 (C_{78}, C_{2v}'), 2.37 (C_{84}, D_2), and 2.65 eV (C_{84}, D_{2d}), which are isomer-dependent and are slightly smaller that that in C_{70}^{2-} (2.745 eV).[13]

The onsite Coulomb repulsion in the three higher fullerene dianions is significantly larger than that evaluated on the basis of the Coulomb repulsion of two point charges localized on the opposite sites of the fullerene cages. The simple Coulomb model (e^2/r) yields repulsion energies of 1.82, 1.80, and 1.73 eV in C_n^{2-} for n = 76, 78, and 84, respectively, using the estimated cage sizes (r) given in ref 17. The same discrepancy was also observed in our previous study on C_{70}^{2-}.[13] The discrepancy reflects the delocalized nature of the two extra electrons, i.e., the wave nature of the electrons. They cannot be viewed as simple classical point charges on the fullerene cages. On the other hand, we found previously that the intramolecular Coulomb repulsion can be estimated via the Coulomb's law in a series of dicarboxylate dianions ($^-O_2C-(CH_2)_n-CO_2^-$, n = 3−10).[31] This is because the two charges are localized at the two ends of the dicarboxylates and they do behave as classical point charges. The large onsite Coulomb repulsion in the fullerene dianions is also a manifestation of strong electron correlation effects, which can lead to shakeup transitions during photodetachment. This effect is observed quite prominently in the low photon energy spectra of C_{70}^{2-} (ref 13) and is also significant in the 532 and 355 nm spectra of C_{76}^{2-}, as revealed by the signals in the band gap region (Figure 1, right column).

4.4. The Repulsive Coulomb Barrier (RCB). One of the fundamental properties of MCAs is the existence of RCB against either electron detachment or charge separation fragmentation.[1−5,25,26] The RCB originates from the superposition of the long-range electron−anion Coulomb repulsion and short-range electron binding. The RCB prevents slow electrons from being emitted

from the dianions during photodetachment and can be estimated from the cutoff in the high binding energy side (low kinetic energies) in the PES spectra.[25,26] The estimated RCBs from the spectral cutoff in the PES of the doubly charged fullerenes are about 1.5, 1.5, and 1.4 eV for C_{76}^{2-}, C_{78}^{2-}, and C_{84}^{2-}, respectively. The magnitudes of the RCBs estimated in the current work are substantially higher than those from the previous PES study (1.10 eV for C_{76}^{2-} and 0.95 eV for C_{84}^{2-}).[17] As demonstrated previously,[31] the RCB can be estimated using classical electrostatic interactions taking into account of the Coulomb repulsion and electron−anion polarization between the leaving electron and the remaining fullerene anion. Taking the reported polarizabilities of C_{76}^{-} (110 Å^3), C_{78}^{-} (114 Å^3), and C_{84}^{-} (127 Å^3),[32] we estimate values of 1.79, 1.76, and 1.71 eV for the RCBs in C_{76}^{2-}, C_{78}^{2-}, and C_{84}^{2-}, respectively, which are in reasonable agreement with the experimentally estimated RCBs on the basis of the PES spectral cutoff. We note that the current RCB for C_{84}^{2-} is consistent with a value (1.74 eV) reported previously using the electrostatic model.[32]

5. Conclusions

We report vibrationally resolved photoelectron spectra of cold higher fullerene singly and doubly charged anions, C_n^{-} and C_n^{2-} ($n = 76, 78, 84$), at several photon energies. The first and second electron affinities of C_{76}, C_{76}, and C_{84} are accurately determined from the 0−0 vibrational transitions in the well-resolved photoelectron spectra. Isomer-specific electron affinities are obtained for C_{78} and C_{84}. Three isomers are observed for C_{78}^{-} and C_{78}^{2-}, and two isomers are observed for C_{84}^{-} and C_{84}^{2-}. The spectra of the dianions are similar to those of the corresponding anions except a shift to lower binding energies by about 2.5−2.6 eV due to the intramolecular Coulomb repulsion in the dianions. The onsite Coulomb repulsions and the repulsive Coulomb barriers for all the doubly charged fullerenes are obtained.

Acknowledgment. We gratefully thank Professor Joe Miller of the University of Utah for providing us the initial sample of TDAE used for the reduction of fullerenes. We also thank Regina Fischer (University of Karlsruhe) for preparation of the neutral fullerene samples used in this study. This work was supported by the U.S. National Science Foundation (CHE-0349426) and the John Simon Guggenheim Foundation and performed at the W. R. Wiley Environmental Molecular Sciences Laboratory, a national scientific user facility sponsored by DOE's Office of Biological and Environmental Research and located at Pacific Northwest National Laboratory, which is operated for DOE by Battelle.

References and Notes

(1) Scheller, M. K.; Compton, R. N.; Cederbaum, L. S. *Science* **1995**, *270*, 1160.

(2) Boldyrev, A. I.; Gutowski, M.; Simons, J. *Acc. Chem. Res.* **1996**, *29*, 497.

(3) Dreuw, A.; Cederbaum, L. S. *Chem. Rev.* **2002**, *102*, 181.

(4) Wang, L. S.; Wang, X. B. *J. Phys. Chem. A* **2000**, *104*, 1978.

(5) Wang, X. B.; Wang, L. S. *Nature* **1999**, *400*, 245.

(6) Martin, R. L.; Ritchie, J. P. *Phys. Rev. B* **1993**, *48*, 4845. Pederson, M. R.; Quong, A. A. *Phys. Rev. B* **1992**, *46*, 13584.

(7) Chang, A. H. H.; Ermler, W. C.; Pitzer, R. M. *J. Phys. Chem.* **1991**, *95*, 9288.

(8) Hettich, R. L.; Compton, R. N.; Ritchie, R. H. *Phys. Rev. Lett.* **1991**, *67*, 1242.

(9) Limbach, P. A.; Schweikhard, L.; Cowen, K. A.; McDermott, M. T.; A. G. Marshall, A. G.; Coe, J. V. *J. Am. Chem. Soc.* **1991**, *113*, 6795.

(10) Herlert, A.; Jertz, R.; Otamendi, J. A.; Martinez, A. J. G.; Schweikhard, L. *Int. J. Mass Spectrom.* **2002**, *218*, 217.

(11) Liu, B.; Hvelplund, P.; Nielsen, S. B.; Tomita, S. *Phys. Rev. Lett.* **2004**, *92*, 168301.

(12) Tomita, S.; Andersen, J. U.; Cederquist, H.; Concina, B.; Echt, O.; Forster, J. S.; Hansen, K.; Huber, B. A.; Hvelplund, P.; Jensen, J.; Liu, B.; Manil, B.; Maunoury, L.; Nielsen, S. B.; Rangama, J.; Schmidt, H. T.; Zettergren, H. *J. Chem. Phys.* **2006**, *124*, 024310.

(13) Wang, X. B.; Woo, H. K.; Huang, X.; Kappes, M. M.; Wang, L. S. *Phys. Rev. Lett.* **2006**, *96*, 143002.

(14) Hampe, O.; Neumaier, M.; Blom, M. N.; Kappes, M. M. *Chem. Phys. Lett.* **2002**, *354*, 303.

(15) Khairallah, G.; Peel, J. B. *Chem. Phys. Lett.* **1998**, *296*, 545.

(16) Ehrler, O. T.; Weber, J. M.; Furche, F.; Kappes, M. M. *Phys. Rev. Lett.* **2003**, *91*, 113006.

(17) Ehrler, O. T.; Furche, F.; Weber, J. M.; Kappes, M. M. *J. Chem. Phys.* **2005**, *122*, 094321.

(18) Wang, X. B.; Woo, H. K.; Wang, L. S. *J. Chem. Phys.* **2005**, *123*, 051106.

(19) Wang, X. B.; Woo, H. K.; Kiran, B.; Wang, L. S. *Angew. Chem., Int. Ed.* **2005**, *44*, 4968.

(20) Wang, X. B.; Yang, X.; Wang, L. S. *Int. Rev. Phys. Chem.* **2002**, *21*, 473.

(21) Subramanian, R.; Boulas, P.; Vijayashree, M. N.; D'Souza, F.; Jones, M. T.; Kadish, K. M. *J. Chem. Soc., Chem. Commun.* **1994**, 1847.

(22) Bauernschmitt, R.; Ahlrichs, R.; Hennrich, F. H.; Kappes, M. M. *J. Am. Chem. Soc.* **1998**, *120*, 5052.

(23) Diederich, F.; Whetten, R. L. *Acc. Chem. Res.* **1992**, *25*, 119.

(24) Achiba, Y.; Kikuchi, K.; Muccini, M.; Orlandi, G.; Ruani, G.; Taliani, C.; Zamboni, R.; Zerbetto, F. *J. Phys. Chem.* **1994**, *98*, 7933.

(25) Wang, X. B.; Ding, C. F.; Wang, L. S. *Phys. Rev. Lett.* **1998**, *81*, 3351 (1998).

(26) Wang, L. S.; Ding, C. F.; Wang, X. B.; Nicholas, J. B. *Phys. Rev. Lett.* **1998**, *81*, 2667.

(27) Haddon, R. C.; Brus, L. E.; Raghavachari, K. *Chem. Phys. Lett.* **1986**, *125*, 459.

(28) Hirsch, A.; Chen, Z. F.; Jiao, H. J. *Angew. Chem., Int. Ed.* **2000**, *39*, 3915.

(29) Echegoyen, L.; Echegoyen, L. E. *Acc. Chem. Res.* **1998**, *31*, 593.

(30) Boltalina, O. V.; Dashkova, E. V.; Sidorov, L. N. *Chem. Phys. Lett.* **1996**, *256*, 253.

(31) Compton, R. N.; Tuinman, A. A.; Klots, C. E.; Pederson, M. P.; Patton, D. C. *Phys. Rev. Lett.* **1997**, *78*, 4367.

(32) Neumaier, M.; Hampe, O.; Kappes, M. M. *J. Chem. Phys.* **2005**, *123*, 074318.